Health Biotechnology and Biopharma (2019), 3(2): 16-39

Original Research Article

In silico docking of matrix metalloproteinase inhibitors of *Hemiscorpius Lepturus* to human matrix metalloproteinases - opportunities for novel natural therapeutics

Mehrdad Ahadi[1], Mahdi Behdani[1], Delavar Shahbazzadeh[1], Fatemeh Kazemi-Lomedasht[1,*]

[1] Biotechnology Research Center, Venom & Biotherapeutics Molecules Laboratory, Pasteur Institute of Iran, Tehran, Iran

***Corresponding author:**. *Fatemeh Kazemi-Lomedasht, Biotechnology Research Center, Venom & Biotherapeutics Molecules Laboratory, Pasteur Institute* of Iran, Tehran, Iran. *Email:* fa_kazemi@pasteur.ac.ir

DOI: 10.22034/HBB.2019.15

Received: April 10, 2019; **Accepted:** May 1, 2019

ABSTRACT

Hemiscorpius Lepturus is one of the most dangerous scorpion species in Iran. Four metalloproteinase inhibitors were detected in the transcriptome of venom gland of *H.lepturus* (HLMetInhibit1, HLMetInhibit2, HLMetInhibit3 and HLMetInhibit4). Their secondary and 3D structures were predicted using Iterative Threading Assembly Refinement (I-TASSER) server. Multiple alignments were performed by clustalW and phylogeny tree constructed using Maximum likelihood statistic method. Phylogeny results showed that, HLMetInhibit1 (MG764541) and HLMetInhibit4 (MG764544) had a different evolutionary pattern than HLMetInhibit2 (MG764542) and HLMetInhibit3 (MG764543). Molecular docking of metalloproteinase inhibitors against the human matrix metalloproteinases (MMPs) were performed using Hex V.8 software. Results showed that HLMetInhibit1 and HLMetInhibit4 had the strongest affinity against almost all human MMPs. The results showed using of the *H.lepturus* metalloproteinase inhibitor as novel human MMPs inhibitors. However, *in silico* finding should be tested in the future *in vitro* studies.

***Keywords*:** Docking, *Hemiscorpius Lepturus*, *in silico*, metalloproteinase inhibitor

INTRODUCTION

The scorpion venom contains the wide-set of materials, which includes types of toxins, proteins and peptides. There are 25 species of scorpion in IRAN that six species of them are toxic [1-3]. One of the most dangerous of these species as point of rate of bit (especially in the cold season) [4] and the number of the deaths [5] is *Hemiscorpius Lepturus*. So far, various compounds were detected in the venom of the *H.lepturus* [6-9]. Transcriptome of venom gland of *H.lepturus* was analyzed by Kazemi-Lomedasht [10]. Early surveys revealed existence of four metalloproteinase inhibitors in the transcriptome of venom gland of *H.lepturus*. Matrix metalloproteinases (MMPs) are endopeptidases that contain zinc and depend on calcium ion [11]. So far, twenty-five kinds of MMPs are recognized [14]. Destruction of kinds of proteins, including extracellular matrix (ECM), cell proliferation, migration, differentiation [15,16], wound healing, angiogenesis and apoptosis are their main functions [17,18]. Matrix metalloproteinase inhibitors (MMPIs) inhibit cell migration and angiogenesis, and are as endogenous and exogenous. Endogenous inhibitors include non-specific type like α2-macroglobulin and specific type like tissue inhibitors of metalloproteinase (TIMPs) [18]. Exogenous inhibitors also include types like peptidomimetic MMPIs, non peptidomimetic MMPIs, tetracycline derivatives and bisphosphonates [19]. Damage in the balance of MMPs and MMPIs leads to increase of MMPs and subsequent occurrence of pathological effects [20]. TIMPs have the critical role in the stability and surviving of ECM [21]. Tissue inhibitors of metalloproteinase (TIMPs) family in vertebrates include four groups (TIMP-1, TIMP-2, TIMP-3 and TIMP-4). In addition, there are four TIMPs in human (HS TIMP-1, 2, 3 and 4) and they have 40 % similarity in their genetic sequence. The most similarity is between TIMP-2 and TIMP-4 (around 50 %), and the less similarity is between TIMP-1 with other TIMPs(37 %) [22].

The human TIMP-1 is able to inhibit most of the MMPs, but its inhibitory function on MT-MMP and MMP 14-16-19-24 is weak. It has two glycosylation sites [23,24]. The human TIMP-2 is mostly as a soluble form [25] and its gene not nested within a syngene [26]. TIMP-2 is unique because it can role as both MMP activator and inhibitor. It also inhibit angiogenesis by inhibiting VEGF-A or FGF-2 [27,28]. The human TIMP-3 is able to inhibit all members of MMPs family, but its most inhibitory tendency is toward the MMP1-2-3 and 9 [29]. It can also inhibit ADAMS, ADAMTS and TNF-a. Its

differentiation point rather than the other members of the family is its ability to connect from N-terminal and the C-terminal domain to extracellular matrix [30]. The human TIMP-3 is the most important *in vivo* regulator for MMPs [31]. Human TIMP-3 has one glycosylation site [23]. Another role of human TIMP-3 is inhibition of angiogenesis. It inhibit angiogenesis by competition with VEGF-A for binding to VEGEFR-2 [32]. Its C-terminal plays the major role in binding to VEGEFR-2 [21,33]. The human TIMP-4 coding gene is located on chromosome 3 and encodes 5 exons [34,35]. Some functional features of four human TIMPs are summarized in Table-1, that extracted from Uniprot and some studies mentioned above [22].

It seems that the above-mentioned category for metalloproteinase inhibitors does not exist in all of the vertebrates. For example, zebrafish (*Danio rera*) has four kinds of TIMP that all of them are similar to human TIMP-2 in their structure. However, there is just an orthologue of mammalian TIMP-3 in cartilaginous fishes [22,36]. These differences are more visible in invertebrates. There is just one TIMP in some of the invertebrates such as *D.melanogaster*, and there are some TIMPs in *Hydra magnipapillata* [37].

Two exogenous metalloproteinase inhibitors named Batimastat and Marimastat have been developed for cancer therapy. Batimastat is the first metalloproteinase inhibitor that its development has been stopped because of low solubility in phase 3 clinical trials [38,39]. In spite of the high efficacy in cancer treatment, dose dependence toxicity, muscular pain and inflammation lead to withdraw of Marimastat in phase 3 clinical trials [40]. Two metalloproteinase inhibitors were isolated from *Didelphis marsupialis* that were able to neutralize snake venom bleeding effects [41]. The metalloproteinase inhibitor named RS_130830 resulted in decrease in the severity of brain damage in meningitis of pneumococcal meningitides [42]. Metalloproteinase inhibitors were able to devastate the biofilm made by *Enterococcus faecalis* [43]. Biardi.et.al showed that the snake venom metalloproteinase inhibitor (SVMPI) in *Spermophilus beecheyi* blood could reduce the MMP activity of Northern Pacific rattlesnake [44]. Palacio et al. in 2017 showed that metalloproteinase inhibitor from the serum of B.*alternatus* could inhibit metalloproteinase (*Batroxase* and *Bjussu* MP-I.) in the snake venom [45]. Four metalloproteinase inhibitors were detected in the transcriptome of venom gland of *H.lepturus*. We named them as

HLMetInhibit1 (MG764541), HLMetInhibit2 (MG764542) HLMetInhibit3 (MG764543) and HLMetInhibit4 (MG764544). Discovering of novel potential therapeutics from the natural sources seems important for treatment of cancer. Therefore, in this study, we performed *in silico* and docking analysis of detected metalloproteinase inhibitors in the transcriptome of *H.lepturus* against human MMPs.

MATERIALS AND METHODS

Bioinformatics analysis

The open reading frames (ORFs) of all metalloproteinase inhibitors were found by ORF finder of NCBI server. Then physical and chemical characteristics of proteins and theoretical PI were determined by Protparam of ExPASy server. The secondary structure of each protein was investigated by Phyre server [46]. The 3D structure was predicted by SWISS-MODEL [47] and I-TASSER [48]. Best predicted structure was selected based on the C-score and QMEAN criterion and saved as PDB file. The 3D structures were observed by Discovery Studio software 2016 [49] and edited by Swiss-PDB Viewer v4.1 [50]. The Binding site of protein was predicted by B-Spred [51] and 3D ligand site web server [52]. Their active site was predicted by COACH servers [53].

Phobius database was used to predict the signal peptide sequence in the protein structure. Protein domain was studied by Prosite server. The glycosylation sites were checked out by NetOGlyc 4.0 Server and NetNGlyc 1.0 Server [54]. BLASTP was performed using NCBI (non-redundant protein sequences) [55] and Uniprot BLAST [56]. BLASTP results were saved as FASTA format. All data was collected in a file and duplicated sequences removed. Using MEGA V.7 software, alignment was performed by clustalW and base on its results phylogeny tree was constructed by Maximum likelihood statistic method (number of bootstrap replications was 500).

The 3D structure of each TIMP1-4 HS and their MMPs target (Table 1) were obtained from RSCB database in PDB format as follows:

(TIMP-1 PDB: 3V96)(TIMP-2 PDB: 1BR9)(TIMP-3 PDB: 3CKI) (MMP-1 PDB: 3AYK)(MMP-2 PDB: 3AYU) (MMP-3 PDB: 2D1O) (MMP-7 PDB: 2MZI) (MMP-8 PDB: 1BZS) (MMP-9 PDB: 5I12) (MMP-10 PDB: 3V96) (MMP-12 PDB: 2MLR) (MMP-13 PDB: 2OW9) (MMP-14 PDB: 3MA2) (MMP-16 PDB: 1RM8).

In cases, that there was not a recorded PBD structure for TIMP or MMP in RSCB, its 3D structure was predicted trough the I-TASSER server. For example: the 3D structures of TIMP-4, MMP-11 ,MMP-15 and MMP-19 was predicted byI-TASSER.

All PDB structures were saved as PDB format (water molecules were removed and polar hydrogens were added) and energy minimized by Swiss-PDB viewer. Ramachandran's map of energy minimized structure was evaluated by PROCHECK interactive server.

Docking analysis

Molecular Docking Analysis was accomplished between receptors (human MMPs) and ligands (Human TIMPs and *H.lepturus* metalloproteinase inhibitors) by Hex V.8 software. Total free energy was calculated using Hex V.8 software (based on the correlation type between electrostatic, and shape parameters) [57]. After each molecular docking, receptor/ligand complex structure was saved as PDB format and amino acid that were involved in interaction identified by LIGPLOT Plus v.1.4.5 [58].

RESULTS

Bioinformatics analysis

The theoretical PI and molecular weight of four metalloproteinase inhibitors of *H.lepturus* determined by Protparam of ExPASy server (Table 2). The 3D structures predicted by I-TASSER and SWISS-MODEL. For each protein the best 3D structure from I-TASSER based on C-score (Table 3) and from SWISS-MODEL based on QMEAN (Table 4) were selected and saved as PDB format. Predicted structures were observed by Discovery Studio2016 (figure 1). Prediction of binding sites of the proteins was performed by B-Spred and 3D ligand site server. The active sites were predicted by Coach Server (Table 5). Results of Phobius server confirmed existence of a signal peptide sequence in metalloproteinase inhibitors of H.*lepturus* except for HLMetInhibit3 (Table 6). Prosite server results showed existence of NTR domain in all proteins. Therefore, their belonging to the TIMPs family was confirmed (Table 6).

The glycosylation site of four proteins was predicted by NetOGlyc 4.0 and NetNGlyc 1.0 servers. Results showed that HLMetInhibit1 and HLMetInhibit4 have O glycosylation sites and HLMetInhibit2 and HLMetInhibit3 have N glycosylation site (Table 7).

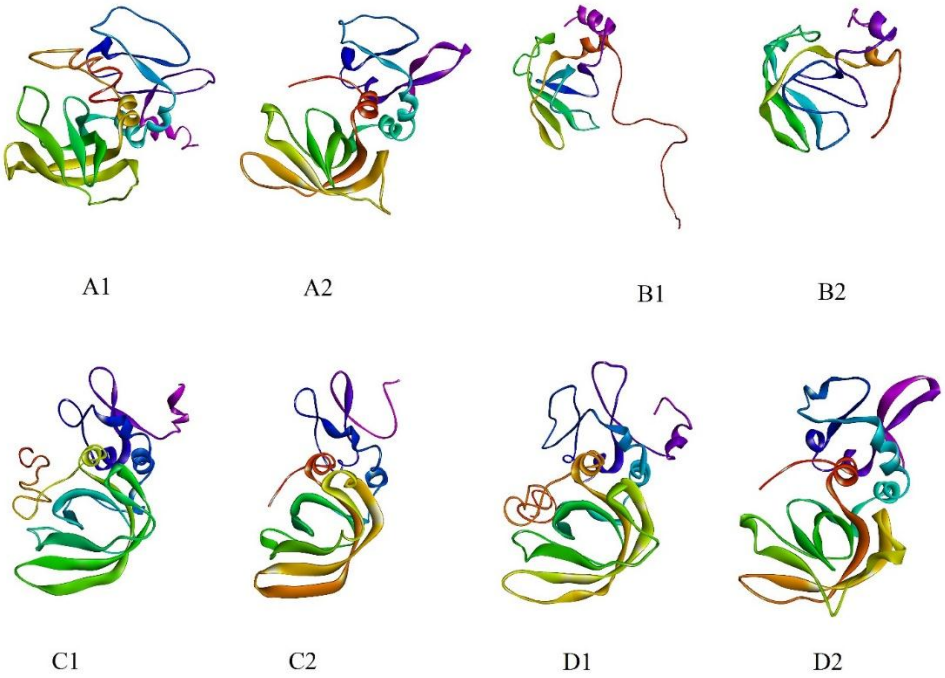

Figure 1. Predicted 3D structure of metalloproteinase inhibitors of *H. lepturus* by I-TASSER and Swiss model Server. (A1) HLMetInhibit1 (MG764541) Predicted by I-TASSER. (B1) HLMetInhibit2 (MG764542) Predicted by I-TASSER. (C1) HLMetInhibit3 (MG764543) Predicted by I-TASSER. (D1) HLMetInhibit4 (MG764544) Predicted by I-TASSER. (A2) HLMetInhibit1 (MG764541) Predicted by Swiss model. (B2) HLMetInhibit2 (MG764542) Predicted by Swiss model. (C2) HLMetInhibit3 (MG764543) Predicted by Swiss model. (D2) HLMetInhibit4 (MG764544) Predicted by Swiss model.

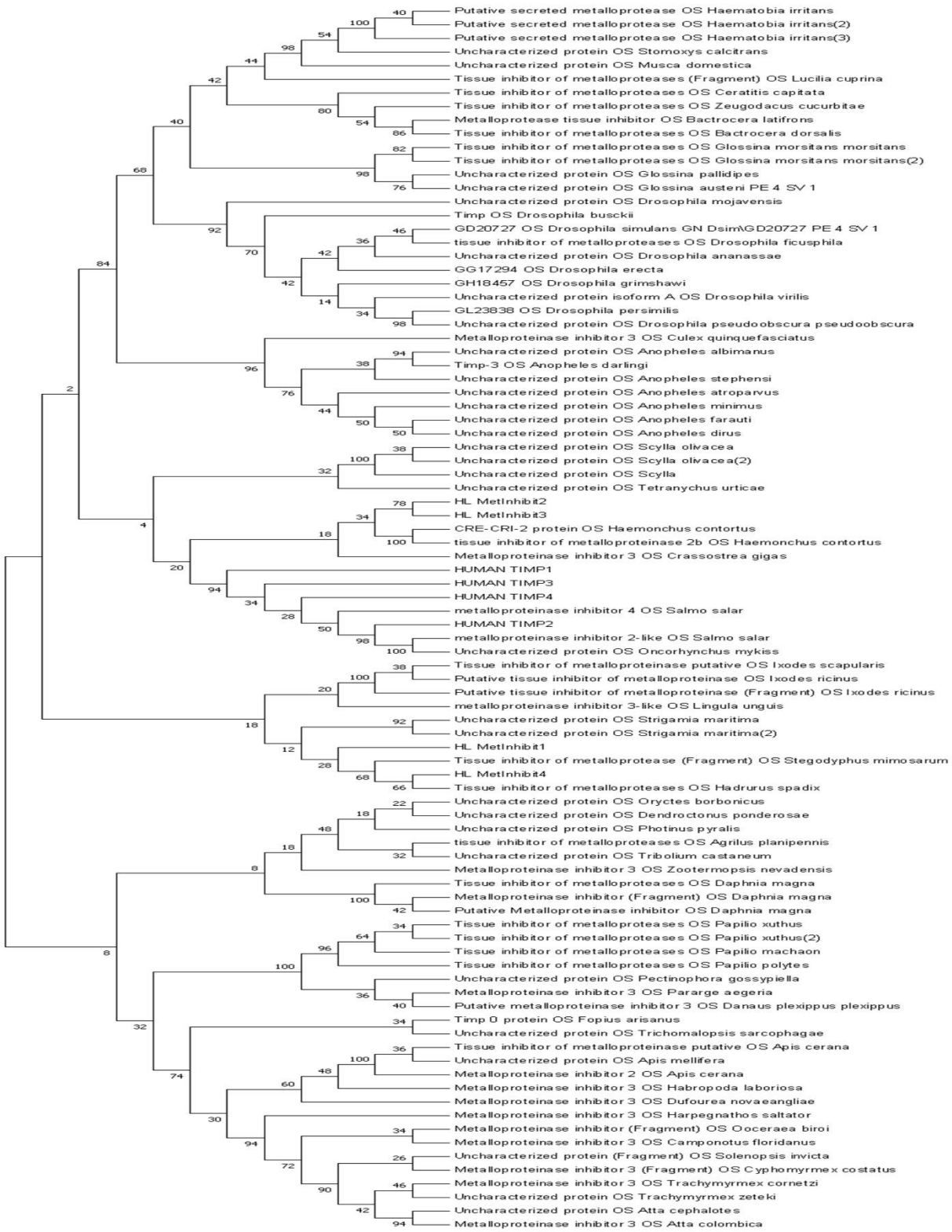

Figure 2. Phylogeny tree of four metalloproteinase inhibitors of *H. lepturus* using Maximum likelihood statistic method. (number of bootstrap replications was 500).

Table 1. Functional features of four human TIMPs, extracted from Uniprot server and some studies

TIMPs Features	Human TIMP-1	Human TIMP-2	Human TIMP-3	Human TIMP-4
UniProt accession ID	KB-P01033	KB-P16035	KB-P35625	KB-Q99727
The inhibitory effect on Human MMPs	**1-2-3-7-8-9-10-11-12-13**	**1-2-3-7-8-9-10-13-14-15-16- 19**	**1-2-3-7-9-10-13-14-15**	**1-2-3-7-9**

Table 2. The chemical futures of metalloproteinase inhibitors of *H. lepturus* predicted by Protparam of ExPASy server

Protein	Residues	Molecular weights Da	pI
HLMetInhibit1 (MG764541)	220	25327.45	**9.95**
HLMetInhibit2 (MG764542)	147	16642.07	**6.41**
HLMetInhibit3 (MG764543)	195	22610.25	**8.42**
HLMetInhibit4 (MG764544)	220	25659.89	**9.71**

Table 3. Features of 3D structures of four metalloproteinase inhibitors of *H.lepturus* predicted by I-TASSER server

Protein	C-score	TM-score	RMSD	Threading template	description
HLMetInhibit1(MG764541)	-0.65	0.63±0.14	6.9±4.1Å	PDB:1uea-Seq ident 21%-Seq coverage 79%	Figure 1, A1
HLMetInhibit2 (MG764542)	-1.10	0.58±0.14	7.0±4.1Å	PDB:3cki-Seq ident 25%-Seq coverage 78%	Figure 1, B1
HLMetInhibit3 (MG764543)	-0.92	0.60±0.14	7.3±4.2Å	PDB:1uea-Seq ident 29%-Seq coverage 80%	Figure 1, C1
HLMetInhibit4 (MG764544)	-0.74	0.62±0.14	7.1±4.2Å	PDB:1uea-Seq ident 26%-Seq coverage 79%	Figure 1 ,D1

Table 4. Features of 3D structures of four metalloproteinase inhibitors of *H.lepturus* predicted by SWISS-MODEL server

Protein	GMQE	QMEAN	Threading template	Description
HLMetInhibit1 (MG764541)	0.52	-6.90	PDB:1buv-Seq ident 36%-seq coverage 77%	Figure 1 ,A2
HLMetInhibit2 (MG764542)	0.47	-8.40	PDB:2tmp-Seq ident 35%- seq coverage 75%	Figure 1, B2
HLMetInhibit3 (MG764543)	0.53	-5.52	PDB:1gxd-Seq ident 35%- seq coverage 81%	Figure 1, C2
HLMetInhibit4 (MG764544)	0.54	-4.29	PDB: 1buv-Seq ident 35%- seq coverage 75%	Figure 1, D2

Table 5. Predicted binding site and active site of metalloproteinase inhibitors of *H.lepturus*

Protein	Prediction site	Prediction Server	Predicted Residues
HLMetInhibit1 (MG764541)	Binding Site	B-Spred	Y 18-H 72-V 152-V 189-R 204-H 205-K 208-R 209-N 210- R 211-A 215
	Binding Site	3DLigandSite	C 24-S 25
	Active Site	COACH	C 24- C 26- H 30- C 36
HLMetInhibit2 (MG764542)	Binding Site	B-Spred	D 56-D 58-R 60-E 69-D 62-A 98-P 132- S 136-N 140-M 141
	Binding Site	3DLigandSite	C 28-S 29-R 92
	Active Site	COACH	A46,G84,I85,V86,S117
HLMetInhibit3 (MG764543)	Binding Site	B-Spred	E 54-D 57-R 60-V 62-L 68-V 124-N 160-K 161-K 174-E 175
	Binding Site	3DLigandSite	C 28-R 29
	Active Site	COACH	C 146-C 148-H 167-C 170
HLMetInhibit4 (MG764544)	Binding Site	B-Spred	L 23-N 195- L 200-K 201-R 206-Q 207-E 211
	Binding Site	3DLigandSite	C 27-S 28
	Active Site	COACH	C 94-C 119- C 144-C 146

Table 6. Prediction of signal peptide sequence and protein domain by Phobius server and Prosite server, respectively

Protein	Signal peptide	Signal peptide location	Domain	Domain location
HLMetInhibit1(MG764541)	Positive	1-19	NTR	24 - 142
HLMetInhibit2(MG764542)	Positive	1- 27	NTR	28 -143
HLMetInhibit3(MG764543)	Negative	--	NTR	28 -146
HLMetInhibit4(MG764544)	Positive	1- 26	NTR	27 - 144

Table 7. Prediction of glycosylation sites in metalloproteinase inhibitors of *H.lepturus* by NetOGlyc 4.0 and netNglyc1.0

Protein	O glycosylation By netOGlyc4.0.0.13	O glycosylation Residue	N glycosylation By netNGlyc1.0	N glycosylation Residue
HLMetInhibit1(MG764541)	#POSITIVE	T 155	#NEGATIVE	--
HLMetInhibit2(MG764542)	#NEGATIVE	--	#POSITIVE	N 102
HLMetInhibit3(MG764543)	#NEGATIVE	--	#POSITIVE	N 49
HLMetInhibit4(MG764544)	#POSITIVE	P 87	#NEGATIVE	--

Phylogeny analysis

To identify the similarity between metalloproteinase inhibitors of H.*lepturus* and same proteins in other species, protein BLAST was performed through NCBI and UniProt servers. According to Uniprot BLAST results, the most similarity of HLMetInhibit1 was with *Stegodyphus mimosarum*-TIMP fragment (Uniprot ID: A0A087TCZ6). The most similarity of HLMetInhibit2, HLMetInhibit3 and HLMetInhibit4 was with *Hadrurus spadix* tissue inhibitor of metalloproteases (Uniprot ID: A0A1W7RA53).

According to BLASTP results of NCBI, the most similarity of HLMetInhibit1 and HLMetInhibit4 was with *Stegodyphus mimosarum*-TIMP fragment (NCBI Accession number: KFM62985.1). The most similarity of HLMetInhibit2 was with *Neodiprion lecontei* PREDICTED: tissue inhibitor of metalloproteases (NCBI Accession number: XP015511793.1). The most similarity of HLMetInhibit3 was with *Parasteatoda tepidariorum* metalloproteinase inhibitor 3-like (NCBI Accession number: XP021001245.1). Then for five most similar results to each protein base on E-value, alignments were performed by both Uniprot and NCBI servers. Conserved amino acid sequences were identified. According to UniProt alignment results, HLMetInhibit1, HLMetInhibit3 and HLMetInhibit4 had12 conserved cysteines and HLMetInhibit2 had five conserved cysteines. According to NCBI multiple alignment, HLMetInhibit1 and HLMetInhibit4 had 11 ,HLMetInhibit2 had 10 and HLMetInhibit3 had 12 conserved cysteine. A total of 90 sequences from Uniprot BLASTP, including four HLMetInhibit sequences and four human TIMPs and 82 sequences for other metalloproteinase inhibitors were used to construct the phylogenetic tree. Phylogeny tree constructed by Maximum likelihood statistic method, using MEGA V.7 software (number of bootstrap replications was 500) (figure 2).

Molecular docking analysis result

Receptors (human MMPs) and ligands (all TIMPs) extracted from PDB and energy minimized by SPDBV (Table 8). The Ramachandra's plot was evaluated by PROCHECK interactive server (Table 9). Molecular docking was performed by HEX v.8 software between TIMPs (Human TIMP1-4 and HLMetInhibit1-HLMetInhibit2-HLMetInhibit3 and HLMetInhibit4) as ligand and human MMPs (MMP1,2,3,7,8,9,10,11,12,13,14,15,16,19) as receptor. Their total free energy

(kcal/mol) were calculated. According to the docking results, HLMetInhibit1 had the highest affinity to MMP-7 and lowest affinity to MMP-16, HLMetInhibit2 had the most affinity to MMP-19 and lowest affinity to MMP-12, HLMetInhibit3 had the most affinity to MMP-11 and lowest affinity to MMP-15 and HLMetInhibit4 had the most affinity to MMP-11 and lowest affinity to MMP-15 (Table 10).

The binding affinity of metalloproteinase inhibitors of *H.lepturus* and TIMP1-4 HS against MMPs were compared (figure 3 and 4). According to docking results, HLMetInhibit1 and HLMetInhibit4 showed the strongest affinity against almost all human MMPs. The average value of all binding affinities for HLMetInhibit4 was -715.14 kcal/mol (aggregate of E.total= -10012.01, divided by the number of MMPs= 14) and for HLMetInhibit1 was -703.81 kcal/mol (aggregate of E.total= 9853.35, divided by the number of MMPs= 14) (Table 10). The complexes with the highest total free energy were selected and their involved amino acids in interaction were evaluated by LIGPLOT Plus software (Table 11) and (figure 5).

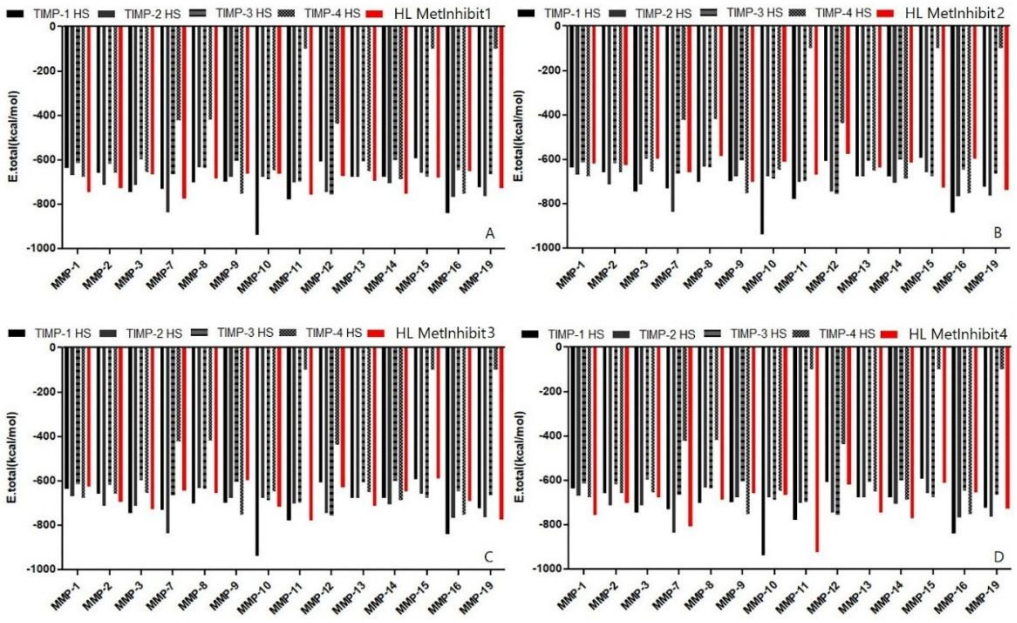

Figure 3. Comparison of binding affinity of metalloproteinase inhibitors of *H.lepturus* and TIMP1-4 HS against human MMPs. (A) HLMetInhibit1 (MG764541). (B) HLMetInhibit2 (MG764542). (C) HLMetInhibit3 (MG764543). (D) HLMetInhibit4 (MG764544).

Table 8. Various minimized energies of the modeled structures in kj/mol

Structures	PDB ID	Bonds	Angles	Torsion	Improper	Non-bonded	Electrostatic	Total	c-score
HLMetInhibit1 (MG764541)	Predicted	207.7	1972.531	2015.59	399.138	-7123.02	-7114.12	-10147.15	-0.65
HLMetInhibit2 (MG764542)	Predicted	271.42	1815.15	1474	373.3	-4360.51	-4573.9	-5008.47	-1.10
HLMetInhibit3 (MG764543)	Predicted	226.15	1875.822	1966.99	439.75	-6280.67	-6087.26	-7884.2	-0.92
HLMetInhibit4 (MG764544)	Predicted	389.28	2675.44	2029.53	433.3	-6945.44	-7820.93	-9228.46	-0.74
Human TIMP-1	3V96	118.49	1155.35	1025.9	156.407	-5450.90	-6485.94	-7386.63	--
Human TIMP-2	1BR9	128.75	983.09	1044.04	161.22	-5960.45	-4036.15	-6779.49	--
Human TIMP-3	3CKI	77.88	690.72	573.16	91.894	-3542.07	-3072.26	-5180.66	--
Human TIMP-4	Predicted	203.93	2122.06	2249.39	405.27	-6825.76	-5643.66	-7488.78	-0.47
Human MMP-1	3AYK	107.9	784.2	799.5	144.3	-4379.5	-4281.2	-6860.87	--
Human MMP-2	3AYU	105.8	1471.9	921.9	414.2	-5839	-2784.1	-5709.3	--
Human MMP-3	2D1O	94.23	1015.89	735.6	125.02	-5680.28	-3504.36	-7213.9	--
Human MMP-7	2MZI	161.76	1713.17	1372.1	238.6	-7946.78	-5100.15	-9561.3	--
Human MMP-8	1BZS	108.52	1067.13	728.35	139	-5690.20	-4715.95	-8364.12	--
Human MMP-9	5I12	80.22	956.86	694.94	132	-5433.87	-2347.25	-5917.16	--
Human MMP-10	3V96	113.45	1011.83	836.54	157-35	-5487.36	-2341.23	-5659.4	--
Human MMP-11	Predicted	510.27	4723.39	4918.36	854.607	-15924.55	-13191.11	-18108.5	0.24
Human MMP-12	2MLR	103.04	1141.76	894.07	157.191	-5448.80	-2450.62	-5603.38	--
Human MMP-13	2OW9	96.67	1046.8	810.59	122.56	-5694.98	-1777.56	-5396.01	--
Human MMP-14	3MA2	5419.2	3064.42	226.83	894.42	-8933.54	-6408.71	-3703.38	--
Human MMP-15	Predicted	906.49	8972.85	9108.67	1780.53	-20121.02	-19484.38	-18836.8	-2.19
Human MMP-16	1RM8	111.27	1067.34	834.58	156.4	-5600.88	-2897.23	-6328.50	--
Human MMP-19	Predicted	472.92	5579.03	5992.08	1108.292	-16430.91	-13924.47	-17132.25	-0.32

Table 9. Ramachandran plot analysis of energy minimized modelled structures evaluated by Ramachandran's map using the PROCHECK interactive server

Protein	PDB ID	Core%	Allowed%	Disallowed%
HLMetInhibit1 (MG764541)	Predicted	59.7%	32.9%	7.4%
HLMetInhibit2 (MG764542)	Predicted	55.6%	36.1%	8.3%
HLMetInhibit3 (MG764543)	Predicted	55.1%	39.9%	5%
HLMetInhibit4 (MG764544)	Predicted	62.3%	35%	2.7%
Human TIMP-1	3V96	87.8%	12.2%	00%
Human TIMP-2	1BR9	88.6%	11.4%	00%
Human TIMP-3	3CKI	87.8%	12.2%	00%
Human TIMP-4	Predicted	69.4%	29.6%	1%
Human MMP-1	3AYK	90.9%	9.1%	00%
Human MMP-2	3AYU	88.2%	11.8%	00%
Human MMP-3	2D1O	90.2%	9.1%	0.7%
Human MMP-7	2MZI	88.4%	9.7%	1.9%
Human MMP-8	1BZS	88.5%	11.5%	00%
Human MMP-9	5I12	90.8%	9.2%	00%
Human MMP-10	3V96	87.8%	12.2%	00%
Human MMP-11	Predicted	66.4%	30.8%	2.8%
Human MMP-12	2MLR	86%	14%	00%

Human MMP-13	2OW9	89.1%	10.2%	0.7%
Human MMP-14	3MA2	88.7%	10.6%	0.7%
Human MMP-15	Predicted	56.5%	38%	5.5%
Human MMP-16	1RM8	92.2%	7.8%	00%
Human MMP-19	Predicted	60%	37.6%	2.4%

Table 10. Various energies of Receptor / Ligand interaction calculated by HEX

	Ligand	**HS TIMP1**	**HS TIMP2**	**HS TIMP3**	**HS TIMP4**	**MetInhibit1 (MG764541)**	**MetInhibit2 (MG764542)**	**MetInhibit3 (MG764543)**	**MetInhibit4 (MG764544)**
Receptor	PDB ID	3V96	1BR9	3CKI	Predicted	Predicted	Predicted	Predicted	Predicted
MMP 1	3AYK	-636.3[a,b]	-670.93	-614.98	-675.2	-745.93	-619.23	-625.18	-755.57
MMP2	3AYU	-659.56	-712.79	-618.04	-658.28	-727.72	-626.38	-695.4	-703.82
MMP3	2D1O	-747.03	-713	-598.77	-654.24	-664.98	-597.28	-726.02	-677.92
MMP7	2MZI	-730.5	-837.94	-664.89	-422.67	-773.9	-658.46	-644.58	-809.01
MMP8	1BZS	-700.89	-631.55	-635.39	-419.08	-685.06	-584.62	-655.24	-689.23
MMP9	5I12	-699.28	-676.27	-604.67	-752.1	-661.65	-700.9	-595.94	-658.88
MMP10	3V96	-936.33	-677.11	-687.46	-649.28	-663.1	-611.81	-715.08	-665.48
MMP11	Predicted	-777.72	-702.69	-697.06	-613.17	-752.78	-670.69	-777.94	-922.69
MMP12	2MLR	-608.67	-743.92	-754.78	-437.81	-671.58	-576.46	-630.45	-617.95
MMP13	2OW9	-677.11	-675.23	-607.95	-649.63	-695.18	-635.81	-712.21	-746.54
MMP14	3MA2	-675.89	-706.11	-599.44	-686.35	-754.04	-614.13	-649.39	-770.16
MMP15	Predicted	-593.84	-657.38	-677.14	-602.11	-679.43	-728.7	-589.61	-612.57
MMP16	1RM8	-840.17	-765.58	-647.26	-751.77	-649.68	-598.3	-692.94	-654.21
MMP19	Predicted	-723.48	-764.2	-665.51	-592.4	-728.32	-738.6	-774.16	-727.98
Aggregate	of E.total	-10006.8	-9934.70	-9073.34	-8568.05	-9853.35	-8961.37	-9484.14	-10012.01
Average	**of E.total**	**-714.77**	**-709.62**	**-648.1**	**-612**	**-703.9**	**-640.1**	**-677.43**	**-715.14**

a: E.total(kcal/mol) ;b: Root mean Squared(RMS) for all docking results was -1

Table 11. Involved amino acid in interaction (between human MMPs and *H.lepturus* metalloproteinase inhibitors)

Interaction Ligand/receptor	**E.total**	**Chain**	**Residues involved in interactions**	**H-Bond**	**Fig**
receptor: MMP 7	-773.9 [a]	A(MMP7)	R241(NE)-L122(O)-K118(O)-R107(NH2,NE)-Y91(OH)-K83(NZ)	7	10-A
Ligand: HLMetInhibit1 (MG764541)		B (HL1)	P220(O)- R136(NE)- Q141(N) -H72(O,O)- N71(ND2)- S219(OG)		
receptor: MMP 19	-738.0	A(MMP19)	S290(O)- S238(OG)- T497(OG1)- T498(OG1)- T280(OG1)	5	10-B
Ligand: HLMetInhibit2 (MG764542)		B (HL2)	Q36(NE2) -K129(O, NZ) -D32(OD2)- G128(O)		
receptor: MMP 11	-777.9	A(MMP11)	S226(OG, OG) –T200(OG1)	3	10-C
Ligand: HLMetInhibit3 (MG764543)		B (HL3)	D75(O)- K133(NZ)- Y185(OH)		
receptor: MMP 11	-922.6	A(MMP11)	S9(OG)- R161(NE, NH2)- D366(O)- R305(NH1)	5	10-D
Ligand: HLMetInhibit4 (MG764544)		B (HL4)	N150(OD1)- H154(NE2)- S172(O)- G91(N)- S92(OG)		

a **(kcal/mol)**

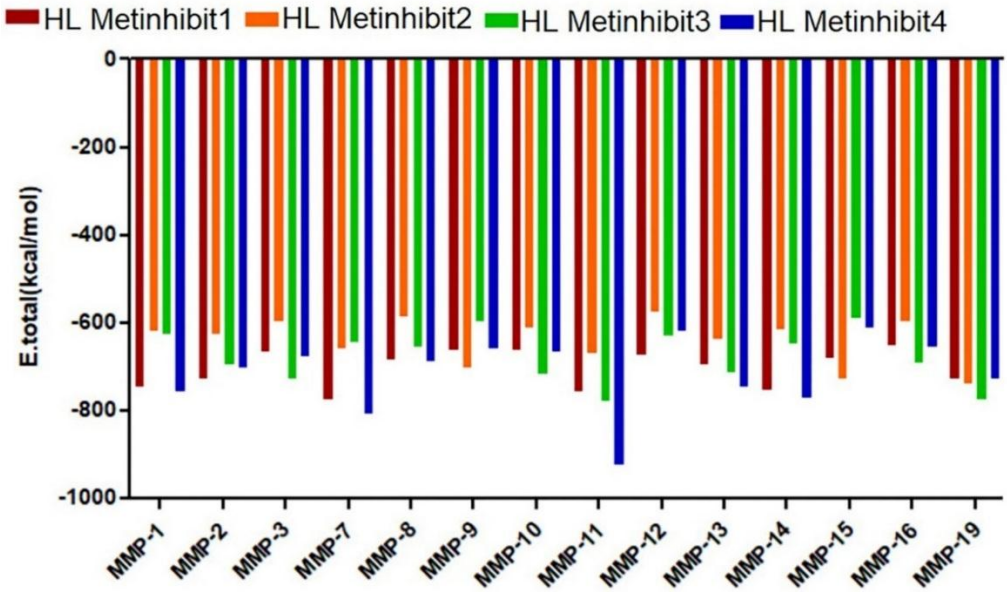

Figure 4. Comparison of binding affinity of metalloproteinase inhibitors of *H.lepturus* against human MMPs. (Red) HLMetInhibit1 (MG764541). (Orange) HLMetInhibit2 (MG764542). (Green) HLMetInhibit3 (MG764543). (Blue) HLMetInhibit4 (MG764544).

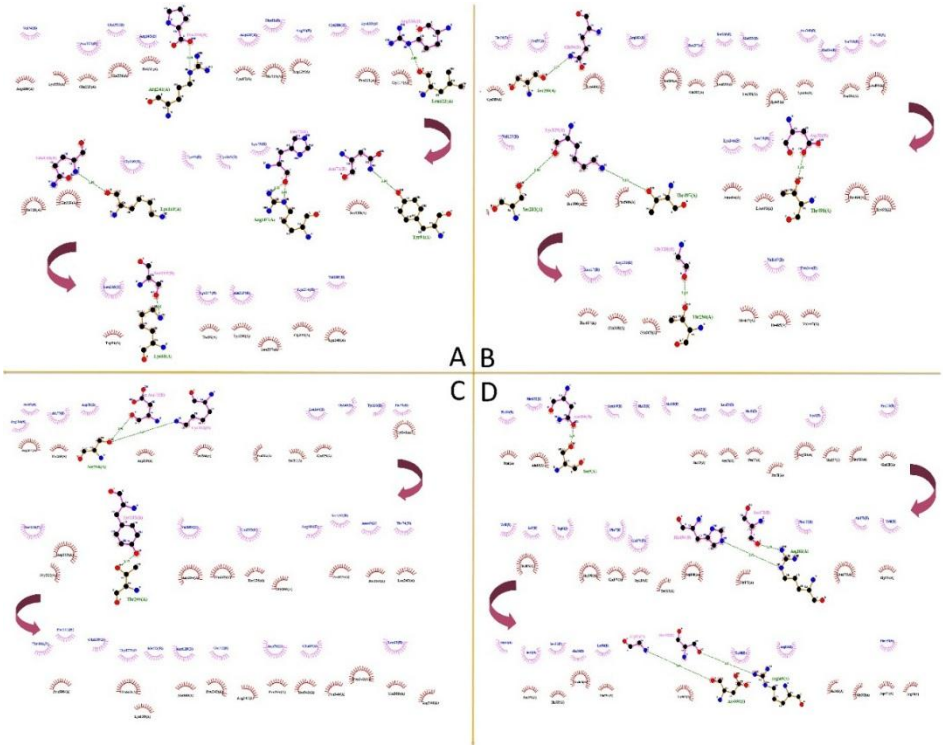

Figure5. Involved amino acids in interactions between receptors and ligands. (A) HLMetInhibit1 (MG764541)/MMP7, (B) HLMetInhibit2 (MG764542)/ MMP19, (C) HLMetInhibit3 (MG764543)/MMP11, (D) HLMetInhibit4 (MG764544)/MMP11.

DISCUSSION

The history of using of animal venom especially scorpion venom as therapeutic related to many years ago. Today, the anti-cancer effect of scorpion venom has been studied in many researches. For example, Jian et.al (2014) showed anti-cancer effect of Iberiotoxin (of *Mesobuthus tamulus* scorpion venom) on MCF-7 breast cancer cells [59]. Inhibitory effect of scorpion venom on motility and colony formation of MDA-MB-231 has been shown by Asmari et.al in 2016 [60]. The venom of *Hemiscorpius lepturus* is very toxic[3]. There are various compounds in the venom of *H.lepturus* with anti-cancer activity. Hemilipin that isolated from the venom of *H.lepturus* showed *in vitro* and *in vivo* inhibitory effect on cancer angiogenesis [9,61]. Anti-angiogenesis activity of Hl-7 and Hl-10 peptides (isolated from *H.lepturus* venom) has been shown by setayesh-mehr et al. [62]. The hemolytic fraction of *H.lepturus* venom named heminecrolysin showed anti-cancer activity on prostate cancer cells (PC-3) [63].

MMP-2 and MMP-9 plays the major function in angiogenesis process. Also, the role of MMP-2 and MMP-9 in the metastasis of breast cancer, especially basal-like triple negative breast cancer has been reported [64,65]. Studies showed that MMP-2 role is more important in expanding of breast cancer [66]. It also has been shown that expression of MMP-11, 14 and 15 was increased in breast cancer tumors [67-69]. Therefore, metalloproteinase inhibitors can play an important role in decreasing cancer progress through inhibition of MMPs and cancer invasion [70].

There are four TIMPs in mammals that each one can inhibit almost all kinds of MMPs [21]. Tissue inhibitor of metalloproteinases have NTR domain (netrin module = NTR; Prosite: PDOC 50189) in N-terminal that is responsible for their inhibitory function on MMPs [71]. There are some differences in structure and the number of TIMPs between invertebrates and mammals. For example, *Drosophila* has one, *Hydra* has three and purple sea urchin has four TIMPs that not correspond to human TIMPs. Nematodes have several genes with one domain for

TIMP that only code a part like N-terminal inhibitor domains of human TIMP [22,37]. In some parasitic helminths, uncommon numbers of TIMPs or NTR domains have been reported. For example, in *Necator Americanos* eight TIMPs and in *Schistosoma haematobium* five NTR domains have been observed [72]. All four TIMPs in mammals have 12 conserved cysteine [73]. Chong-Chong Gao et al. showed that metalloproteinase inhibitor can induce apoptosis of pancreatic cancer cells [74]. Zhang et.al showde that increasing expression of TIMP-3 in prostate cancer cell reduce angiogenesis and induce apoptosis [75].

Primary studies on transcriptome analysis showed that there are four metalloproteinase inhibitors in *H.lepturus* venom. We named them as HLMetInhibit1 (MG764541), HLMetInhibit2 (MG764542), HLMetInhibit3 (MG764543) and HLMetInhibit4 (MG764544). HLMetInhibit1 and HLMetInhibit2 had 220, HLMetInhibit3 had 195 and HLMetInhibit4 had 147 amino acids length. HLMetInhibit1, 2 and 4 had a signal peptide sequences but HLMetInhibit3 did not have. All of them had a NTR domain in their N-terminal. HLMetInhibit1 and HLMetInhibit4 had one O glycosylation site, HLMetInhibit2 and HLMetInhibit3 had N glycosylation site. HLMetInhibit1, HLMetInhibit3 and HLMetInhibit4 had 12 conserved cysteine residues. Phylogeny analysis showed that HLMetInhibit1 and HLMetInhibit4 have different evolutionary pattern than HLMetInhibit2 and HLMetInhibit3. Comparisons of four HLMetInhibits with human TIMPs reveal that, HLMetInhibit2 and HLMetInhibit3 were more similar to human TIMPs in their evolutionary pattern. Molecular docking results showed that HLMetInhibit1 had the most binding affinity with MMP-7 and the least binding affinity with MMP-16. Six amino acid (P220- R136- Q141 -H72- N71- S219) and seven hydrogen bonds are involved in its receptor/ligand interaction. HLMetInhibit2 had the most binding affinity with MMP-19 and the least binding affinity with MMP-12. Four amino acid (Q36 -K129-D32-G128) and five hydrogen bonds are involved in its receptor/ligand interaction. HLMetInhibit3 had the most binding affinity with MMP-11 and the least binding affinity with MMP-15. Three amino acids (D75- K133- Y185) and three hydrogen bonds are involved in its receptor/ligand interaction. Finally, HLMetInhibit4 had the most binding affinity with MMP-11 and the least binding affinity with MMP-15. Five amino acid (N150- H154- S172- G91- S92)

and five hydrogen bonds are involved in its receptor/ligand interaction.

CONCLUSION

Molecular docking results showed a similar binding affinity pattern of HLMetInhibit1 and HLMetInhibit4 compare to human TIMP-1 and TIMP-2 (Table 10). I-TASSER prediction pattern for HLMetInhibit1 and HLMetInhibit4 is Tissue inhibitor of metalloproteinase-1 (1UEA) (Table3) and Swiss homology modeling pattern for HLMetInhibit1 and HLMetInhibit4 is tissue inhibitor of metalloproteinases-2 (1BUV) (Table4). In addition, there are a structure similarity between HLMetInhibit1 and HLMetInhibit4 and human TIMPs in number of conserved cysteine residues. The *in silico* results promise for further evaluation of all HLMetInhibits specially HLMetInhibit1 and HLMetInhibit4 in *in vitro* studies and potentiate for consideration and development as novel natural therapeutics.

ACKNOWLEDGMENT

We thank Pasteur Institute of Iran, Tehran, Iran.

REFERENCES

[1]. Vega RCR, Schwartz EF, Possani LD. Mining on scorpion venom biodiversity. *Toxicon*, 2010; 56(7):1155-61.

[2]. Abdel-Rahman MA, Quintero-Hernández V, Possani LD. Scorpion venom gland transcriptomics and proteomics: an overview. *Venom Genomics Proteomics*, 2016: 105-24.

[3]. Pipelzadeh M.H, Jalali A, Taraz M, Pourabbas R, Zaremirakabadi A. An epidemiological and a clinical study on scorpionism by the Iranian scorpion Hemiscorpius lepturus. *Toxicon*, 2007; 50(7): 984-92.

[4]. Kassiri H , Kasiri N, Dianat A. Species composition, sex ratio, geographical distribution, seasonal and monthly activity of scorpions and epidemiological features of scorpionism in Zarrin-dasht County, Fars Province, Southern Iran. *Asian Pac J Tro Dis*, 2015; 5: 99-103.

[5]. Borchani L, Sassi A, Gharsa HB, Safra I, Shahbazzadeh D, Lasfar ZB, El Ayeb M.The pathological effects of Heminecrolysin, a dermonecrotic toxin from Hemiscorpius lepturus scorpion venom are mediated through its

lysophospholipase D activity. *Toxicon*, 2013; 68: 30-39.

[6]. Shahbazzadeh D, Srairi-Abid N, Feng W, Ram N, Borchani L, Ronjat M, Akbari A, Pessah IN, De Waard M, El Ayeb M. Hemicalcin, a new toxin from the Iranian scorpion Hemiscorpius lepturus which is active on ryanodine-sensitive Ca2+ channels. *Biochem J*, 2007; 404(1): 89-96.

[7]. Srairi-Abid N, Shahbazzadeh D, Chatti I, Mlayah-Bellalouna S, Mejdoub H, Borchani L, Benkhalifa R, Akbari A, El Ayeb M. Hemitoxin, the first potassium channel toxin from the venom of the Iranian scorpion Hemiscorpius lepturus. *FEBS J*, 2008; 275(18): 4641-50.

[8]. Borchani L, Sassi A, Shahbazzadeh D, Strub JM, Tounsi-Guetteti H, Boubaker MS, Akbari A, Van Dorsselaer A, El Ayeb M. Heminecrolysin, the first hemolytic dermonecrotic toxin purified from scorpion venom. *Toxicon*, 2011; 58(1): 130-39.

[9]. Jridi I, Catacchio I, Majdoub H, Shahbazeddah D, El Ayeb M, Frassanito MA, Ribatti D, Vacca A, Borchani L. Hemilipin, a novel Hemiscorpius lepturus venom heterodimeric phospholipase A2, which inhibits angiogenesis in vitro and in vivo. *Toxicon*, 2015; 105: 34-44.

[10]. Kazemi-Lomedasht F, Khalaj V, Bagheri KP, Behdani M, Shahbazzadeh D. The first report on transcriptome analysis of the venom gland of Iranian scorpion, Hemiscorpius lepturus. *Toxicon*, 2017; 125: 123-30.

[11]. Vanlaere I, Libert C. Matrix metalloproteinases as drug targets in infections caused by gram-negative bacteria and in septic shock. *Clin Microbiol Rev*, 2009; 22(2): 224-39.

[12]. Cao J, Sato H, Takino T, Seiki M. The C-terminal region of membrane type matrix metalloproteinase is a functional transmembrane domain required for pro-gelatinase A activation. *J Biol Chem*, 1995; 270(2): 801-805.

[13]. Fanjul-Fernández M, Folgueras AR, Cabrera S, López-Otín C. Matrix metalloproteinases: evolution, gene regulation and functional analysis in mouse models. *Biochimi Biophys Acta*, 2010; 1803(1): 3-19.

[14]. Birkedal-Hansen H, Moore WG, Bodden MK, Windsor LJ, Birkedal-Hansen B, DeCarlo A, Engler JA. Matrix metalloproteinases: a review. *Crit Rev Oral Biol Med*, 1993; 4(2): 197-250.

[15]. Mott JD, Werb Z. Regulation of matrix biology by matrix

metalloproteinases. *Curr Opin Cell Biol*, 2004; 16(5): 558-64.

[16]. Egeblad, M. Werb Z. New functions for the matrix metalloproteinases in cancer progression. *Nature Rev Cancer*, 2002; 2(3): 161-74.

[17]. Gill SE, Parks WC. Metalloproteinases and their inhibitors: regulators of wound healing. *Int J Biochem Cell Biol*, 2008; 40(6): 1334-47.

[18]. Löffek S, Schilling O, Franzke CW. Biological role of matrix metalloproteinases: a critical balance. *Eur Respi Soc*, 2011:191-208.

[19]. Yang JS, Lin CW, Su SC, Yang SF. Pharmacodynamic considerations in the use of matrix metalloproteinase inhibitors in cancer treatment. *Expert Opin Drug Metab Toxicol*, 2016; 12(2): 191-200.

[20]. CT Palei A, P Granger J, E Tanus-Santos J. Matrix metalloproteinases as drug targets in preeclampsia. *Curr Drug Targets*, 2013; 14(3): 325-34.

[21]. Qi JH , Ebrahem Q, Ali M, Cutler A, Bell B, Prayson N, Sears J, Knauper V, Murphy G, Anand-Apte B. Tissue inhibitor of metalloproteinases-3 peptides inhibit angiogenesis and choroidal neovascularization in mice. *PLoS One*, 2013; 8(3): 55667.

[22]. Brew K, Nagase H. The tissue inhibitors of metalloproteinases (TIMPs): an ancient family with structural and functional diversity. *Biochimi Biophys Acta*, 2010; 1803(1): 55-71.

[23]. Murphy G.Tissue inhibitors of metalloproteinases. *Genome Biol*, 2011; 12(11): 233.

[24]. Docherty AJ, Lyons A, Smith BJ, Wright EM, Stephens PE, Harris TJ, Murphy G, Reynolds JJ. Sequence of human tissue inhibitor of metalloproteinases and its identity to erythroid-potentiating activity. *Nature*, 1985; 318(6041): 66-69.

[25]. Hammani K, Blakis A, Morsette D, Bowcock AM, Schmutte C, Henriet P, DeClerck YA. Structure and characterization of the human tissue inhibitor of metalloproteinases-2 gene. *J Biol Chem*, 1996; 271(41): 25498-505.

[26]. Jaworski DM, Beem-Miller M, Lluri G, Barrantes-Reynolds R. Potential regulatory relationship between the nested gene DDC8 and its host gene tissue inhibitor of metalloproteinase-2. *Physiol Genomics*, 2007; 28(2): 168-78.

[27]. Bourboulia D, Stetler-Stevenson WG. Matrix metalloproteinases (MMPs) and tissue inhibitors of metalloproteinases (TIMPs): Positive and negative regulators in tumor cell adhesion. *Semin Cancer Biol*. 2010: 20 (3): 161-68.

[28]. Stetler-Stevenson WG, Krutzsch HC, Liotta LA. Tissue inhibitor of metalloproteinase (TIMP-2). A new member of the metalloproteinase inhibitor family. *J Biol Chem*, 1989; 264(29): 17374-78.

[29]. Anand-Apte B, Bao L, Smith R, Zetter B, Iwata K, Olsen BR, Apte SS. A review of tissue inhibitor of metalloproteinases-3 (TIMP-3) and experimental analysis of its effect on primary tumor growth. *Biochem Cell Biol*, 1996; 74(6): 853-62.

[30]. Lee MH, Atkinson S, Murphy G. Identification of the extracellular matrix (ECM) binding motifs of tissue inhibitor of metalloproteinases (TIMP)-3 and effective transfer to TIMP-1. *J Biolo Chem*, 2007; 282(9): 6887-98.

[31]. Nagase H, Visse R, Murphy G. Structure and function of matrix metalloproteinases and TIMPs. *Cardiovasc Res*, 2006; 69(3): 562-73.

[32]. Qi JH, Ebrahem Q, Moore N, Murphy G, Claesson-Welsh L, Bond M, Baker A, Anand-Apte B. A novel function for tissue inhibitor of metalloproteinases-3 (TIMP3): inhibition of angiogenesis by blockage of VEGF binding to VEGF receptor-2. *Nat Med*, 2003; 9(4): 407-15.

[33]. Apte SS, Olsen BR, Murphy G. The gene structure of tissue inhibitor of metalloproteinases (TIMP)-3 and its inhibitory activities define the distinct TIMP gene family. *J Biol Chem*, 1995; 270(24): 14313-18.

[34]. Olson TM, Hirohata S, Ye J, Leco K, Seldin MF, Apte SS. Cloning of the human tissue inhibitor of metalloproteinase-4 gene (TIMP4) and localization of the TIMP4 and Timp4Genes to human chromosome 3p25 and mouse chromosome 6, respectively. *Genomics*, 1998; 51(1): 148-51.

[35]. Leco KJ, Apte SS, Taniguchi GT, Hawkes SP, Khokha R, Schultz GA, Edwards DR. Murine tissue inhibitor of metalloproteinases—4 (Timp—4): cDNA isolation and expression in adult mouse tissues. *FEBS Lett*, 1997; 401(2-3): 213-17.

[36]. Putnam NH, Srivastava M, Hellsten U, Dirks B, Chapman J, Salamov A, Terry A, Shapiro H, Lindquist E, Kapitonov VV, Jurka J. Sea anemone genome reveals

ancestral eumetazoan gene repertoire and genomic organization. *Science*, 2007; 317(5834): 86-94.

[37]. Brew K, Dinakarpandian D, Nagase H. Tissue inhibitors of metalloproteinases: evolution, structure and function. *Biochimi Biophys Acta*, 2000; 1477(1): 267-83.

[38]. Cathcart J, Pulkoski-Gross A, Cao J. Targeting matrix metalloproteinases in cancer: Bringing new life to old ideas. *Genes Dis*, 2015; 2(1): 26-34.

[39]. Gialeli C, Theocharis AD, Karamanos NK. Roles of matrix metalloproteinases in cancer progression and their pharmacological targeting. *FEBS J*, 2011; 278(1): 16-27.

[40]. Coussens LM, Fingleton B, Matrisian LM. Matrix metalloproteinase inhibitors and cancer—trials and tribulations. *Science*, 2002; 295(5564): 2387-92.

[41]. Neves-Ferreira AG, Cardinale N, Rocha SL, Perales J, Domont GB. Isolation and characterization of DM40 and DM43, two snake venom metalloproteinase inhibitors from Didelphis marsupialis serum. *Biochimi Biophys Acta*, 2000; 1474(3): 309-20.

[42]. Liechti FD, Bächtold F, Grandgirard D, Leppert D, Leib SL. The matrix metalloproteinase inhibitor RS-130830 attenuates brain injury in experimental pneumococcal meningitis. *J Neuroinflammation*, 2015; 12(1): 43.

[43]. Tay CX, Quah SY, Lui JN, Yu VS, Tan KS. Matrix metalloproteinase inhibitor as an antimicrobial agent to eradicate *Enterococcus* faecalis biofilm. *J Endod*, 2015; 41(6): 858-63.

[44]. Biardi J, Ho CY, Marcinczyk J, Nambiar KP. Isolation and identification of a snake venom metalloproteinase inhibitor from California ground squirrel (*Spermophilus beecheyi)* blood sera. *Toxicon*, 2011; 58(6): 486-93.

[45]. Palacio TZ, Santos-Filho NA, Rosa JC, Junior RS, Barraviera B, Sampaio SV. Isolation and characterization of a novel metalloprotease inhibitor from Bothrops alternatus snake serum. *Int J Biol Macromol*, 2017; 98: 436-46.

[46]. Kelley LA, Mezulis S, Yates CM, Wass MN, Sternberg MJ. The Phyre2 web portal for protein modeling, prediction and analysis. *Nat Protoc*, 2015; 10: 845.

[47]. Biasini M, Bienert S, Waterhouse A, Arnold K, Studer G, Schmidt T, Kiefer F, Cassarino TG, Bertoni M, Bordoli L, Schwede T. SWISS-MODEL: modelling protein tertiary and quaternary structure

using evolutionary information. *Nucleic Acids Res*, 2014; 42(1): 252-58.

[48]. Yang J, Yan R, Roy A, Xu D, Poisson J, Zhang Y. The I-TASSER suite: protein structure and function prediction. *Nat Methods*, 2015; 12(1): 7-8.

[49]. BIOVIA DS, BIOVIA Discovery Studio 2017 R2: A comprehensive predictive science application for the Life Sciences. San Diego, CA, USA , 2017.

[50]. Guex N, Peitsch MC. SWISS-MODEL and the Swiss-Pdb Viewer: an environment for comparative protein modeling. *Electrophoresis*, 1997; 18(15): 2714-23.

[51]. Mukherjee S, Zhang Y. Protein-protein complex structure predictions by multimeric threading and template recombination. *Structure*, 2011; 19(7): 955-66.

[52]. Wass MN, Kelley LA, Sternberg MJ. Predicting ligand-binding sites using similar structures. *Nucleic Acids Res*, 2010; 38(2): 469-73.

[53]. Yang J, Roy A, Zhang Y. Protein–ligand binding site recognition using complementary binding-specific substructure comparison and sequence profile alignment. *Bioinformatics*, 2013; 29(20): 2588-95.

[54]. Blom N, Sicheritz-Pontén T, Gupta R, Gammeltoft S, Brunak S. Prediction of post-translational glycosylation and phosphorylation of proteins from the amino acid sequence. *Proteomics*, 2004; 4(6): 1633-49.

[55]. Altschul SF, Madden TL, Schäffer AA, Zhang J, Zhang Z, Miller W, Lipman DJ.Gapped BLAST and PSI-BLAST: a new generation of protein database search programs. *Nucleic Acids Res*, 1997; 25(17): 3389-3402.

[56]. Consortium U. UniProt: the universal protein knowledgebase. *Nucleic Acids Res*, 2017; 45(1): 158-69.

[57]. Ghoorah AW, Devignes MD, Smaïl-Tabbone M, Ritchie DW. Protein docking using case-based reasoning. *Proteins Struct Funct Bioinformat*, 2013; 81(12): 2150-58.

[58]. Laskowski RA, Swindells MB. Multiple ligand–protein interaction diagrams for drug discovery. *ACS Publications*, 2011: 2778-86.

[59]. Ding J, Chua PJ, Bay BH, Gopalakrishnakone P. Scorpion venoms as a potential source of novel cancer

therapeutic compounds. *Exp Biol Med*, 2014; 239(4): 387-93.

[60]. Al‐Asmari A K, Islam M, Al‐Zahrani AM. In vitro analysis of the anticancer properties of scorpion venom in colorectal and breast cancer cell lines. *Oncol Lett*, 2016; 11(2): 1256-62.

[61]. Jridi I, Catacchio I, Majdoub H, Shahbazzadeh D, El Ayeb M, Frassanito MA, Solimando AG, Ribatti D, Vacca A, Borchani L. The small subunit of Hemilipin2, a new heterodimeric phospholipase A2 from Hemiscorpius lepturus scorpion venom, mediates the antiangiogenic effect of the whole protein. *Toxicon*, 2017; 126: 38-46.

[62]. Setayesh-Mehr Z, Asoodeh A. The inhibitory activity of HL-7 and HL-10 peptide from scorpion venom (Hemiscorpius lepturus) on angiotensin converting enzyme: Kinetic and docking study. *Bioorg Chem*, 2017; 75: 30-37.

[63]. Shahbazzadeh D, Yardehnavi N, Kazemi-Lomedasht F, Bagheri KP, Behdani M. Anticancer activity of H. lepturus venom and its hemolytic fraction (heminecrolysin). *Heal Biotechnol Biopharma*. 2017; 1: 46-53.

[64]. Mehner C, Hockla A, Miller E, Ran S, Radisky DC, Radisky ES. Tumor cell-produced matrix metalloproteinase 9 (MMP-9) drives malignant progression and metastasis of basal-like triple negative breast cancer. *Oncotarget*, 2014; 5(9): 2736.

[65]. Bhattacharyya N, Mondal S, Ali MN, Mukherjee R, Adhikari A, Chatterjee A. Activated salivary MMP-2-A potential breast cancer marker. *Open Conf Proc J*. 2017; 8(1).

[66]. Radenkovic S, Konjevic G, Jurisic V, Karadzic K, Nikitovic M, Gopcevic K. Values of MMP-2 and MMP-9 in tumor tissue of basal-like breast cancer patients. *Cell Biochem Biophys*, 2014; 68(1): 143-52.

[67]. Gonzalez L, Pidal I, Junquera S, Corte MD, Vazquez J, Rodriguez JC, Lamelas ML, Merino AM, Garcia-Muniz JL, Vizoso FJ. Overexpression of matrix metalloproteinases and their inhibitors in mononuclear inflammatory cells in breast cancer correlates with metastasis-relapse. *Br J Cancer*, 2007; 97(7): 957-63.

[68]. Perentes JY, Kirkpatrick ND, Nagano S, Smith EY, Shaver CM, Sgroi D, Garkavtsev I, Munn LL, Jain RK, Boucher Y. Cancer cell–associated MT1-MMP

promotes blood vessel invasion and distant metastasis in triple-negative mammary tumors. *Cancer Res*, 2011; 71(13): 4527-38.

[69]. McGowan P, Duffy M. Matrix metalloproteinase expression and outcome in patients with breast cancer: analysis of a published database. *Ann Oncol*, 2008; 19(9): 1566-72.

[70]. Radisky ES, Sarmazdeh MR, Radisky DC. Therapeutic potential of matrix metalloproteinase inhibition in breast cancer. *J Cell Biochem*, 2017; 118(11): 3531-48.

[71]. Bányai L, Patthy L. The NTR module: domains of netrins, secreted frizzled related proteins, and type I procollagen C-proteinase enhancer protein are homologous with tissue inhibitors of metalloproteases. *Protein Sci*, 1999; 8(8): 1636-42.

[72]. Cantacessi C, Hofmann A, Pickering D, Navarro S, Mitreva M, Loukas A. TIMPs of parasitic helminths–a large-scale analysis of high-throughput sequence datasets. *Parasit Vectors*, 2013; 6(1): 156.

[73]. Hayakawa T. Tissue inhibitors of metalloproteinases and their cell growth-promoting activity. *Cell Struct Funct*, 1994; 19(3): 109-14.

[74]. Gao CC, Gong BG, Wu JB, Cheng PG, Xu HY, Song DK, Li F. MMI-166 a selective matrix metalloproteinase inhibitor, promotes apoptosis in human pancreatic cancer. *Med Oncol*, 2015; 32(1): 1-9.

[75]. Zhang L, Zhao L, Zhao D, Lin G, Guo B, Li Y, Liang Z, Zhao XJ, Fang X. Inhibition of tumor growth and induction of apoptosis in prostate cancer cell lines by overexpression of tissue inhibitor of matrix metalloproteinase-3. *Cancer Gene Ther*, 2010; 17(3): 171-79.